Reliability-Based Casing Design for Geothermal Wells

Hans Petter Lohne[1], Jan Aage Aasen[2], Erlend Randeberg[1], Hans Joakim Skadsem[1]

[1] NORCE Norwegian Research Centre, Prof. Olav Hanssensvei 15, 4021 Stavanger, Norway

[2] University of Stavanger, Kjølv Egelands hus, Kristine Bonneviesvei 22, 4021 Stavanger, Norway

halo@norceresearch.no

Keywords: Reliability, casing design, risk analysis, well integrity, three-dimensional well tubular design.

ABSTRACT

The main subsurface structural components of geothermal wells are casing strings, liners and the annulus cement between the formation and casings, and between successive casing strings. In high temperature geothermal wells in particular, casings, tubulars and connections will be exposed to significant loads due to production-related temperature changes in the well. Such significant loads combined with possible reductions in the mechanical integrity of the casing caused by exposure to elevated temperatures or corrosive formation fluids, means that casing failure becomes an important environmental and economic risk in high temperature geothermal wells.

Casing programs for oil and gas wells and for geothermal wells are traditionally based on the working stress design approach, where minimum strength requirements of the casing are determined by comparing casing strength to the magnitude of severe accidental loads that may occur during the lifetime of the well. Uncertainties in the load and strength of the casing are accounted for by design factors that are mostly based on experience and do not reflect the probability or consequence of the different casing failure modes. This approach may result in overly conservative casing designs, or design requirements for high temperature wells that are difficult to meet without expensive, high-end tubulars.

In this paper we discuss reliability-based design as an alternative approach for geothermal casing design. Reliability-based design is a stochastic approach to design where uncertainties in loads and material properties are considered explicitly by assigning probability distributions to uncertain parameters that affect stresses and material strength. The casing design is now based on quantitative failure probabilities associated with different modes of failure for different design alternatives, allowing more risk-consistent designs compared to traditional working stress designs. We illustrate the principles of reliability-based design on an example high temperature geothermal well and compare the design to an equivalent working stress design.

The mechanistic model utilized in the paper is three-dimensional (3D) by nature (triaxial). It consists of calculating the von Mises stress (effective stress) from radial, tangential and axial stresses. Loading cases include changes in pressure, temperature and mechanical stress. The yield limit is displayed as a circle. Note that hydrostatic stress (volume change) does not impact von Mises stress, while deviatoric stress (shape change) does change this effective stress.

1. INTRODUCTION

Reliable wells for deep geothermal energy are key to economical and environmentally friendly harvesting of thermal resources abundantly available in the earth's crust. Long-life performance becomes an ever more challenging issue as higher temperature wells are targeted by the industry, as illustrated e.g. by the Icelandic Deep Drilling Project (IDDP) initiative. High reservoir temperatures, large temperature variations between phases of production and well interventions, and corrosive well fluids impose large thermal stresses and chemical loads on subsurface components. The primary components are casings, liners and the annulus cement between the formation and casings, and between successive casings. Integrity of these is essential to maintain well integrity, i.e. prevent unintended annular migration of formation fluids. In addition, the structural components should provide mechanical borehole stability and isolate lost-circulation zones encountered while drilling.

The basis for selecting casing strings for a given well is created through a casing design process, which can follow different approaches. These approaches will be explained in section 3 and discussed in section 5 in the context of an example case presented in section 4. In an attempt to keep the writing and ideas in this paper clear and concise, the focus will be on 3D well tubular design for casing strength. Analyzed load case is that of thermal axial loading of cemented casing.

Industry standard equation 42 in API RP 5C3 (2018) is not the same as the one found in ISO/TR 10400 (2018), despite their otherwise similar content. The latter's version of the equation does not include the effect of inside pressure, while the equation in the first expresses the exact effect of inside pressure. The exact triaxial description (3D well tubular design) of collapse pressure under axial stress and internal pressure was included by API in 2015 as Annex M, with official updating of equation 42 three years later. The present paper explores the updated standard formulation from API in a casing design context.

The new API equation 42 has already produced alternative hydrocarbon design methods that are more accurate than the old. Goodman et al. (2018) presented exact yield ellipse for burst pressure and exact yield ellipse for collapse pressure, while Aasen et al. (2017) used the same exact theory expressed as a symmetric yield circle. The 3D well tubular design model presented herein is an enhancement of the 2017 method, as uniaxial collapse pressure is now replaced by equivalent triaxial collapse pressure.

2. CASING CHALLENGES

Challenges associated with casing failures can be considered in view of relevant failure modes and their severity. The casing strings are key barrier elements and emphasis should be made to ensure proper selection of casing for a given well design.

Well barrier failure modes can be general or specific in their description, often depending on the variety of the elements or equipment they apply to. Failure modes can be standardized for certain areas of application, such as the standard ISO 14224 (2016), which is used to collect reliability data for oil and gas equipment. A failure mode can be viewed as being between the cause of a failure and the consequence of the failure, as it does not necessarily provide information about why the failure occurred or what it may lead to, only how the failure materializes.

Casing failure modes can be categorized as follows:

- Leakage
- Material degradation, including different types of corrosion
- Burst/rupture
- Bulge/collapse
- Buckling
- Plugged or choked flow
- Breakdown
- Spurious displacement/slippage

Several of these modes are strongly interconnected and partly consequences of each other.

There is little published information describing failure rates of geothermal wells. However, as reported by Davies et al. (2014), rates are expected to vary significantly due to the wide range of geological settings from which geothermal energy can be exploited, e.g. volcanically active regions and tectonically quiescent regions. Teodoriu (2015) investigated the root causes of casing failures when exposing the string to thermal and chemical loads, highlighting different casing fatigue mechanisms seen especially in geothermal wells. As ever higher temperature resources are targeted, even supercritical well fluids are encountered, leading to more frequent well failures, of which the casing is a key element that may fail (Kruszewski and Wittig 2018). Thereby, the casing program is probably the most crucial single factor for ensuring successful longevity of a geothermal well.

3. DESIGN APPROACHES

The main objective of casing design is to find a design that enables the well to fulfill its function throughout its design life. This means that the casing must be strong enough to withstand the loads it will be subjected to, without resulting in a failure. This is analysed by identifying failure modes of concern and modelling their occurrence. The difference between approaches are primarily in terms of the modelling.

The three main approaches to design are Working Stress Design (WSD), Limit State Design (LSD) and Reliability Based Design (RBD). The main differences between these approaches are in how detailed they try to model failure. WSD traditionally only analyse the elastic region and does not investigate plastic behaviour. LSD allows the design to approach its ultimate strength, meaning the plastic region is investigated (strain-based design). While WSD tend to use nominal values and LSD use minimal values, both rely on design safety factors (or design factors for short) to account for uncertainty in assumptions and values. RBD approaches can be performed in various ways, but the essence is to investigate the effect of uncertainty in assumptions and values on the probability of casing failure. In the following subsections WSD is described in terms of a triaxial model and how RBD can be performed.

3.1 Working Stress Design (WSD)

WSD relies on a design factor (DF) to ensure safety in the design. This factor is equal to the strength divided by the load, or more specifically to how it is used here, equal to the material yield strength divided by the total equivalent triaxial (von Mises) stress. The selection of DFs has often been based on past experience or common practice rather than calculations. Table 1 refers numbers suggested in some standards and typical ranges used by oil & gas companies. For 3D well tubular design loads all seem to suggest a DF of 1.25. This means that load subjected to the tubular should be maximum 80% of its minimum yield strength, rendering a margin to compensate for error in design equations and loading estimates.

Table 1: Design factors for casing based on NZS 2403:2015, NORSOK D-010, and Smith and Miller (2009)

	Burst	Collapse	Axial	Triaxial
NZS 2403 (2015)	1.50-1.80	1.20	1.00-1.80	1.25
NORSOK D-010 (2013)	1.10	1.10	1.25	1.25
Typical oil operator range (Lewis and Miller 2009)	1.00-1.25	1.00-1.10	1.30-1.90	1.25

Table 5 in NZS 2403 (2015) lists design factors for a total of ten load cases, which is why these are represented by a range in Table 1. These load cases include the triaxial stress condition, which is the focus of this paper, as well as four axial stress conditions and five hoop stress (pressure differential) conditions (three internal and two internal pressure conditions).

The varying design factors (from DF = 1 to 1.8) could be a reflection of uncertainty in regard to load resistance and the load itself. The lowest DF is for helical buckling in uncemented casing. The design equations used for this case are well established and the load case is clearly defined. The highest DF occurs for both axial and hoop stress conditions. Using different design factors for different load cases are typical for LSD, and not WSD.

To focus on WSD, in the following developments we assume that the pipe material does not exceed its yield strength. The combination of inside pressure, outside pressure and axial stress dictates any well design, and a triaxial stress model is therefore pursued.

In the present paper we use a standard oilfield solution published by API TR 5C3 (2018) where equations for triaxial yield of pipe body are discussed in Annex A. The yield circle is defined as shown in Figure 1, where A_O is the area within the circumference of the pipe, A_s is the cross-sectional area of the pipe steel, p_i is the internal pressure, p_o is the external pressure, σ_a is the axial stress, σ_n is the neutral axial stress and σ_y is the yield stress of the pipe.

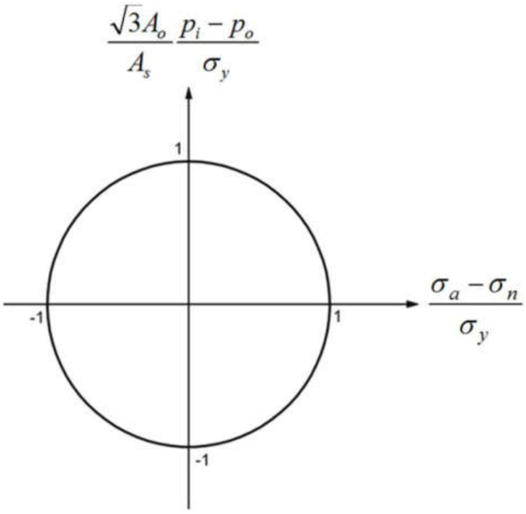

Figure 1: Dimensionless yield circle adapted from API TR 5C3 (2018).

At the circle itself (unit radius) the von Mises stress is equal to the yield strength of the tubular material. Inside the circle the pipe is stressed below yield, while outside the circle the tubular is stressed beyond its yield strength. At the center of the circle we observe that all three principal stresses are the same and the von Mises stress is zero. The equation for the yield circle is shown below. It is 100% exact and yet so simple.

$$x^2 + y^2 = 1 \qquad [1]$$

Equation [1] is applicable for a large variety of calculations for straight and buckled pipe. It is valid as long as the combined stresses in the pipe (from force, buoyed self-weight and pressure differential) does not exceed the yield strength of the material.

The neutral axial stress was derived by Woods in a written discussion published as a part of the ground-breaking paper by Klinkenberg (1951):

$$\sigma_n = \frac{\sigma_t + \sigma_r}{2} = \frac{A_i p_i - A_o p_o}{A_s} \qquad [2]$$

Sparks (1984) presented the effective force F_E as a function of real force F_R and two pressure-area loads:

$$F_E = F_R + A_o p_o - A_i p_i \qquad [3]$$

Substituting $F_R = A_s\sigma_a$, it follows that $F_E = A_s(\sigma_a - \sigma_n)$ and the observation that the x-coordinate for the circle is the dimensionless effective force.

The working stress design of cemented geothermal casing is fairly straightforward assuming that the casing steel is prevented from expanding when heated. Instead of expanding the casing is compressed thermally when heated. For vertical depth coordinate $z = 0$ at the bottom, the effective thermal force is expressed for all depth values as follows (negative sign means compression):

$$F_{Et}(z) = -EA_s\alpha\Delta T(z) \qquad [4]$$

Here E is Young's modulus, α is the linear thermal expansion coefficient and ΔT is the temperature change. The total effective force in the production casing is a combination of its initial condition (hanging weight in wet cement) and thermal compression (during hot production). Initial axial effective force in the casing, as the cement cures:

$$F_{Ei}(z) = wz \qquad [5]$$

The buoyed unit weight w (unit is N/m) follows from Lubinski et al. (1962):

$$w = w_s + A_i\rho_i g - A_o\rho_o g \qquad [6]$$

The total effective force for a cemented geothermal casing is $F_{Ei} + F_{Et}$:

$$F_E(z) = wz - EA_s\alpha\Delta T(z) \qquad [7]$$

Using the yield circle, we write:

$$\Delta p = \frac{\sqrt{3}A_s}{3A_o}\sqrt{\sigma_y^2 - \frac{F_E^2}{A_s^2}} \qquad [8]$$

Equation [7] predicts the allowable pressure differential for given yield strength and loading. If $F_E/A_s \geq \sigma_y$, then all available strength is consumed by axial stress and there is no available pressure differential.

This equation is valid for burst (all pipe sizes) and for yield collapse (thick-walled pipe). For a freely hanging submerged tubular, we know that the effective force (buoyed weight) at bottom is zero.

Industry standard for oilfield casing is to calculate collapse pressures from the API design equations (API TR 5C3, 2018). These equations are limited to zero axial stress and zero outside pressure. Devised adjustment for axial stress and internal pressure is as follows ($\sigma_a + p_i \geq 0$):

$$\frac{\sigma_{y*}}{\sigma_y} = \sqrt{1 - \frac{3(\sigma_a+p_i)^2}{4\sigma_y^2}} - \frac{\sigma_a+p_i}{2\sigma_y} \quad [9]$$

This is the newly introduced equation 42 in API TR 5C3 (2018). The adjustment by API takes place in the bottom right quadrant in Figure 1. In the present paper the bottom left quadrant is also adjusted for effects on collapse for axial stress and internal pressure.

It is stated by API that this equation is not valid for σ_{y*} less than 24 000 psi (165 MPa), which is a limit that is relevant for the analysis presented below. It is a known fact that for increasing casing size the collapse resistance is reduced. For example, comparing the nominal API collapse pressures for 9⅝" 53.5 lbs/ft casing and 13⅜" 72 lbs/ft casing, the greater size collapse pressure is 40% of that of the smaller size. It is evident that tubular with high diameter-to-thickness ratio is indeed capable of producing σ_{y*} less than 24 000 psi (165 MPa).

The discussed API limitation means that the presented methodology cannot be used for low σ_{y*}. This happens for very thin-walled tubular members. The presented WSD is not valid for elastic collapse (the extreme thin-walled API collapse case) and this is not a surprise since the collapse pressure is a function of Young's modulus and Poisson's ratio, but not related to yield strength for such very thin-walled tubular members. For example, for the production casing presented in section 4 we obtain σ_{y*} = 372 MPa and remain well within API limitation.

For heated casing in cemented geothermal wells the axial stress is compressive, and we get $\sigma_a + p_i < 0$. Deploying equation [8], we observe a beneficial effect since σ_{y*}/σ_y is greater than one. The API standard does not incorporate the beneficial effect of compression for pipe collapse even though this relation is firmly established by the yield circle.

Lubinski (1975) derived the following exact relationship between yield strength and loading:

$$\frac{2A_o(p_o-p_i)}{A_s\sigma_y} = \sqrt{1 - \frac{3(\sigma_a+p_i)^2}{4\sigma_y^2}} - \frac{\sigma_a+p_i}{2\sigma_y} \quad [10]$$

Comparing equations 9 and 10 we observe that:

$$\sigma_{y*} = \frac{2A_o(p_o-p_i)}{A_s} \quad [11]$$

To calculate casing collapse using the circle we deploy σ_{y*} instead of σ_y. The pressure differential in equation [11] is the API nominal collapse pressure. The meaning of nominal collapse in this context is to consider zero inside pressure and zero axial stress. This value is tabulated in drilling engineering handbooks or can be calculated from standard API equations (API TR 5C3, 2018).

Equation [11] calculates equivalent yield strength based on standard API collapse pressures. We use σ_y for calculating burst, while for collapse we use σ_{y*}. For collapse of thick-walled pipe, it follows that σ_{y*} is equal to σ_y. For this category of tubulars, it follows that triaxial burst resistance is equal to triaxial collapse resistance.

It is easily shown that equation [11] in fact is the standard yield strength collapse pressure equation (thick-wall). This is equation (35) in section 8.4.2 in both API RP 5C3 (2018) and ISO/TR 10400 (2018) expressed in a different manner.

For thin-walled pipe, the nominal collapse resistance is lower than predicted by yielding. The transition from thick-wall (analytical yield collapse pressure) to thin-wall (experimental collapse pressure) takes place for diameter-to-thickness ratio equal to a value between 12 and 15, depending upon the yield strength of the tubular material.

For thin-walled pipe, the WSD method used herein is to perform 3D well tubular design by expressing the nominal API collapse pressure (obtained experimentally for axial zero stress and zero internal pressure) as equivalent yield strength. For API plastic collapse, transition collapse and elastic collapse we observe increasingly reduced collapse resistance and therefore reduced values of σ_{y*}/σ_y. Structural instability becomes more important as diameter-to-thickness ratio increases, while at the same time the material yield strength becomes less important.

If for tubular of interest we choose to plot the circle using pressure differential versus effective stress as coordinates, the circle for σ_{y*} (thin-wall collapse) will be smaller than the circle for σ_y (burst and thick-wall collapse). If the pipe collapses by yielding (thick-walled pipe), the two circles are identical. The same information is displayed if the dimensionless circle with radius equal to one is deployed for design calculations. In this case the dimensionless stress vector from origin (hydrostatic stress) to loading (deviatoric stress) will be greater for σ_{y*} than for σ_y.

Adjusting the yield strength of the casing material for the effect of temperature is important in geothermal well design. In the present paper we use Table 4 from the New Zealand code of practice for deep geothermal wells (NZS 2403, 2015) to adjust the API yield strength for the effect of temperature. The burst and collapse calculations are the same as for nominal API yield strength, with the exception that the yield strength is reduced according to the casing temperature at given depth.

3.2 Reliability Based Design (RBD)

Nominal values are used for the casing properties when following a WSD approach, while relying on design factors to account for uncertainty in model and parameters. Experiments referred to in (API TR 5C3, 2018) show there is significant uncertainty related to the manufacturing and material of casings. Based on many experiments performed by casing manufacturers, this uncertainty in e.g. casing outer diameter and wall thickness and material yield strength, has been quantified using probability distributions to represent the uncertainty.

Models for RBD can be developed in various ways, such as accounting for uncertainty in both load and design strength, only strength, as a function of time or as a basis for selecting design factors. How the RBD is developed depends on what it will be used for. For example, Maes et al. (1995) provides an example where load and resistance factor design (LFRD) were used to determine reasonable design factors that ensures that the design will have reliability better than a certain threshold when used with design check equations. Das and Samuel (2015) discussed how changes occur over time and how RBD can be performed by simulating the life of a well as a series of operations.

The model used here to illustrate RBD is simply utilization of the same model described for WSD, but with “actual” parameters obtained from a representative population of casings instead of nominal parameters. This means that the RBD performs a Monte Carlo simulation by sampling the probability distributions representing the population of casing parameters and using them in the model. The parameters treated as uncertain are the casing outer diameter, wall thickness and yield strength. This influences the magnitude of A_o, A_s and σ_y, as well as the calculation of $p_o - p_i$. Note that in the calculation of $p_o - p_i$ the nominal values for the empirical parameters is used, and not the “actual” value.

This implementation of RBD does not include uncertainty in load or other assumptions than those mentioned, which should be kept in mind for the discussion.

4. EXAMPLE CASE

Table 2 shows the geothermal well example studied. Heating of a 9⅝" production casing that is cemented in place is the load case considered. We are concerned with the change of temperature – from the time when the cement has just cured (hardened) to the time of steady-state production.

Table 2: Overview of input parameters for 9⅝" 53.5 lbs/ft production casing example case.

Parameter	Value
Casing diameter	0.2445 m (9.625")
Wall thickness	0.0138 m (0.545")
Diameter/thickness	17.66
Casing weight w_s	780.8 N/m (53.5 lbs/ft)
Grade	L80
Yield strength (NZS 2403:2015)	293 K: 552 MPa (80 000 psi) 473 K: 496 MPa (72 000 psi)
API nominal collapse pressure	45.64 MPa (6620 psi)
Fluid density during casing cementing	1000 kg/m3 inside casing 1800 kg/m3 outside casing
Buoyed casing weight w	314.2 N/m (21.53 lbs/ft)
Casing depth	1000 m
Linear change in casing temperature while cement cure	100 K (100 °C) at casing shoe 150 K (150 °C) at surface
Steady-state linear casing temperature	473 K (200 °C) regardless of depth
Young’s modulus	206.8 GPa
Thermal expansion coefficient	$12 \cdot 10^{-6}$ K^{-1}
Gravitational acceleration	9.80665 m/s^2

The total effective force profile shown is the starting point for both WSD and RBD. Figure 2 shows the effective axial force profiles initially (blue) and during steady-state hot production (red) plus the combined effects of the two (green).

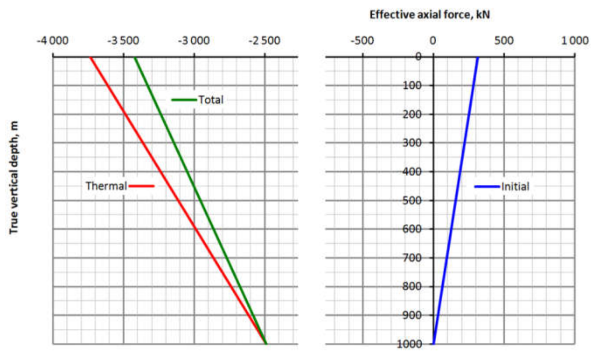

Figure 2: Axial force profiles for initial condition (hanging tension in wet cement), hot production (thermal compression) and combined loading.

During cementing the casing is freely suspended at the surface. The buoyancy factor w/w_s is equal to 0.40, which means that the submerged casing weighs 40% of its dry weight. The reason for the relatively high amount of buoyancy (low value of buoyancy factor) is that there is cement outside and water inside the casing. The hanging weight is 314 kN shown as the top point of the initial force profile (blue line). At bottom the effective axial force (buoyed weight) is zero. If the real axial force profile were to be shown, the top point would be the same as for effective axial force while the bottom point would be compression (buoyancy force acting on bottom).

Axial compression created by thermal expansion is directly proportional to the temperature increase in the cemented casing. At surface we see that the thermal stress is at its highest absolute value since the temperature change is greatest here. An important observation is that the thermal loading is one order in magnitude greater than the initial loading.

The overall loading is the combined effects of initial tension and thermal compression, leading to total axial loading on surface that is about 90% of thermal loading. At bottom of the casing the initial effective force (hanging self-weight) is zero, which means that there is no reduction in overall loading.

A consequence of manifested thermal stresses is that the burst and collapse pressures are reduced. This is evident by inspecting equation [8]. The higher amount of loading (increased F_E squared), the less strength is available in the casing to deal with pressure differential.

Figure 3 shows two set of curves. Collapse is to the left and burst to the right. For the solid lines there is no yield strength reduction at elevated temperature. For the dashed lines the yield strength is adjusted according to temperature adjustment coefficients in NZS 2403 (2015).

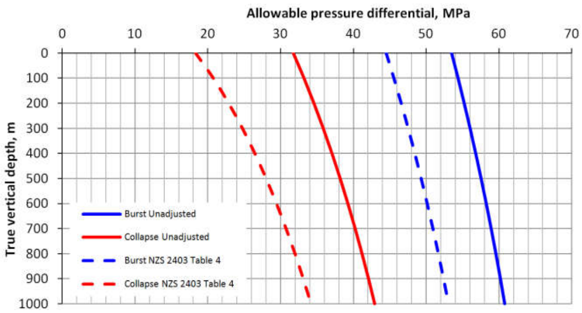

Figure 3: Allowable pressure differential with and without temperature adjustment.

Observe that the collapse resistance is less than the burst resistance since diameter-to-thickness ratio is greater than 15. The resistance to pressure differential is lowest near the surface. There is a significant reduction in pressure differential resistance if the yield strength of the casing steel is adjusted for well temperature. The reduction in collapse pressure caused by the thermal yield strength adjustment is greater than calculated for burst pressure.

The RBD approach could be made more detailed but will in this example be restricted to the same equations used for WSD, but with distributions replacing the nominal values. This is done for the outer diameter of the casing, the thickness, and the yield strength. The distributions used to replace the nominal values are ensemble values provided in tables F.3 and F.4 in ISO/TR 10400 (2018) for L80 grade casings. These are based on a large number of samples from different manufacturers. The distribution for yield strength relative to the nominal value have a mean of 1.10 and covariance of 0.0529 as seen in Figure 4.

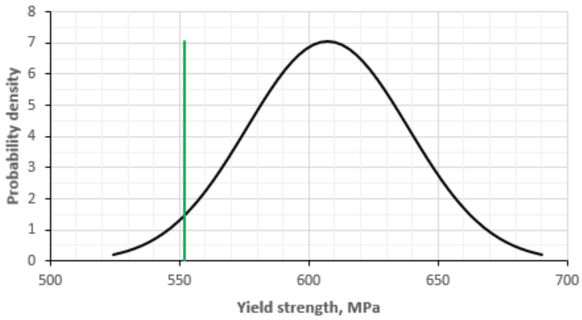

Figure 4: Distribution of yield strength (black) for L80 grade casing compared to the nominal value (green)

Distributions for outer diameter and wall thickness likewise have means 1.0059 and 1.0069 and covariances 0.00181 and 0.0259 respectively. Ovality, eccentricity and residual stress have not been considered.

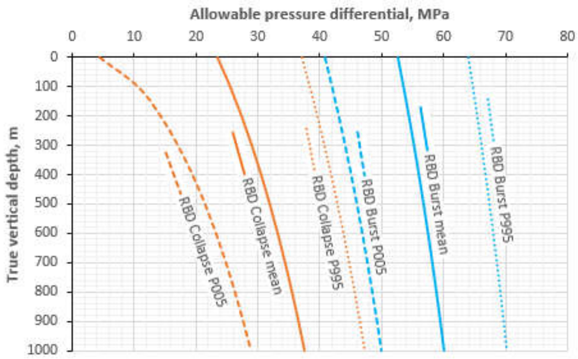

Figure 5: Allowable pressure differential when reflecting the uncertainty in yield strength, outer diameter and wall thickness.

Figure 5 shows six curves that has been produced by the RBD approach while adjusting for the effect of temperature on yield strength. The light blue curves on the right represent the pressure differential allowable for burst, while the orange curves are for collapse. The RBD approach produces distributions, which is reflected by the dotted curves representing the 99.5 percentile of the distribution (P995) and the dashed curves representing the 0.5 percentile (P005). In other words, there is a 0.5% probability, under the assumptions made, that there will be less than the allowable pressure differential represented by the orange dashed line available for collapse.

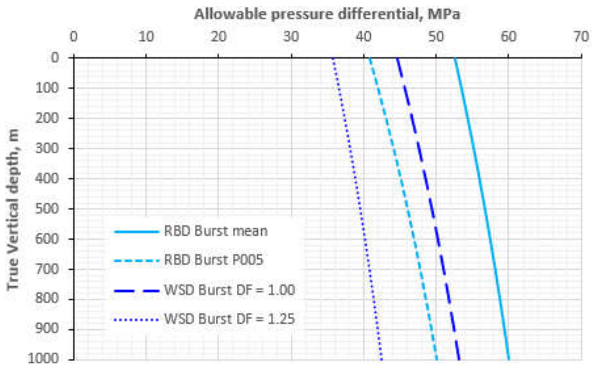

Figure 6: Comparison between WSD with without adjustment for design factor and mean and 0.5 percentile of RBD for burst

Figure 6 compares the RBD results for burst shown in Figure 5 with the from the WSD approach shown in Figure 4, as well as what would be allowed with a design factor of 1.25. It can be observed that WSD with DF = 1.25 provides a reasonable result when compared to the statistical foundation.

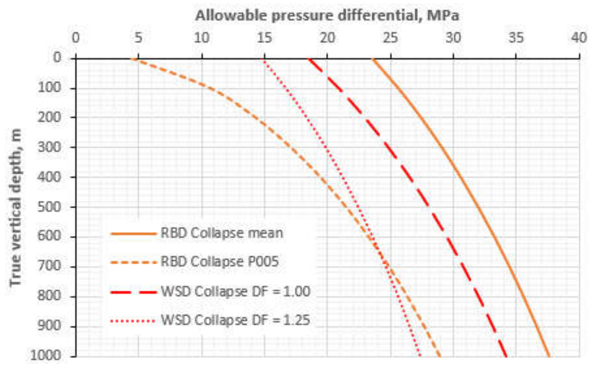

Figure 7: Comparison between WSD with and without adjustment for design factor and mean and 0.5 percentile of RBD for collapse

Figure 7 shows the same comparison as Figure 6, but for collapse. The use of the WSD appears less conservative in this comparison, with the design factored line being higher than the minimum RBD line at most depths.

Single percentile numbers are usually poor representations of the uncertainty represented by the full distribution. Figure 8 therefore shows the distribution from the RBD approach at the surface and compares it to the WSD values at this depth. The probability of being below the WSD value with DF = 1.0 is about 19%, while when adjusting for a DF of 1.25 it is reduced to about 7%

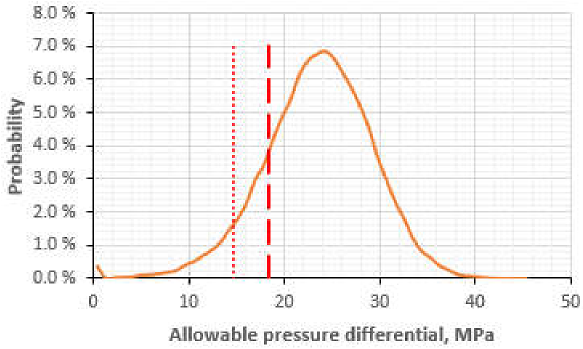

Figure 8: Allowable pressure differential for collapse at surface for RBD (orange), WSD with DF = 1.0 (red dashes) and WSD with DF = 1.25 (red dots)

5. DISCUSSION

Thus far we have presented the WSD and RBD approaches and exemplified them on a case. The RBD approach followed has been kept simple and has not included any detailed stochastic modelling. The RBD results presented have not been intended to provide a foundation for casing design, but to illustrate the essence in the benefit of RBD over WSD by focusing on the underlying assumptions that lie within the use of design factors.

As seen in Table 1, the design factors vary between sources, where the geothermal standard NZS 2403 (2015) uses larger design factors for burst and collapse. This is reasonable given that high thermal axial loads are common in geothermal wells, which will use up a fair bit of the casing strength as seen in the triaxial model. However, it also illustrates that the design factors should depend on the conditions the casings will be used in.

The New Zealand code of practice for geothermal wells suggests a design factor of 1.25 for triaxial loads, as does all other casing design suggestions in Table 1. Comparing the use of nominal values in the triaxial model and the result using a distribution for some of these parameters give some insight into what these design factors indicate.

Figure 6 showed that for burst the design factor and conservative nominal values makes sure that the design criteria is well into the tail of the RBD distribution. For collapse, as seen in Figure 7 and Figure 8, the results in the example are not as conservative, with a 7% probability that the RBD value is lower than the WSD value adjusted with the design factor. This is much more than the what is usually considered as target reliability levels. Although all the uncertainty associated with casing design is not accounted for in the RBD results, where conservativeness in values and the central limit theorem indicates that doing so will not necessarily increase the probability, it still gives further evidence that a WSD approach is not consistent in its treatment of uncertainty.

The difference between burst and collapse is the use of API experimental values (thin-walled tubular) for collapse that is different than one would obtain using yield ellipse equations (thick-walled tubular). It is worth noting that the sources for the design factors in Table 1 does not state which exact models should be used together with the design factors, as the sources they refer to include several models for the same failure modes. The result of the design approach will therefore depend on which model is used, which should be reflected in the design factor. The standards provide estimates for the accuracy of different models they provide for collapse, the uncertainty in the model can be reflected in an RBD approach. Note that because most of the models are on the conservative side (when compared with the API sample data), a failure may not exist even if the pressure differential should exceed what is set as allowable.

As seen in Figure 4, the nominal values for casings are usually conservative. However, table F.2 in ISO/TR 10400 (2018) illustrate that the manufacturing has a large influence on the variance in casing properties. The representative distributions differ between different manufacturers, where some are more or less conservative and have larger or smaller variance in the properties of their products. Quality can also improve over time, as new technologies are taken into use. Such aspects are only included in an RBD approach, where proper value can be put on paying for higher quality products (or settle for less). Advice on how to determine distributions for casing properties for samples sizes, as well as how to perform RBD based on them, is given in ISO/TR 10400 (2018) Annex F.

This work has mostly focused on modelling of the resistance to loads in casings, and not on the loads themselves. As mentioned when presenting Table 1, different design factors can be used for different load conditions. This can be a method to compensate for how unlikely some of the loads that drive the design can be, and is usually associated with limit state design. The main difference between limit state design and working stress design, however, is usually considered to be the evaluation of stresses beyond the elastic range. LSD is typically considered necessary for viable designs when conditions are particularly difficult. In the oil & gas industry there are typically some accidental loads, loads that are preventable but might happen anyway with a low probability, that dominate the needs of the design. Operational loads, on the other hand, put less constraint on the design. This makes the advice by Lewis and Miller (2009) to use WSD for operational loads and LSD for accidental loads reasonable.

Due to the high temperature many geothermal wells exploit, the temperature related loads become dominating. Temperature expansion of the steel, for example, can easily drive the design requirements and make designs within yield impracticable. These loads would be operational, not accidental, and the argument that the design should only survive the load, not necessarily be suitable for repeated occurrences, may therefore not be valid in these cases. For very high temperature wells another practice is to use strain-based design as described by Droessler et al. (2017), which could be considered LSD or RBD depending on how the uncertainty is treated. Introducing new design elements, such as the flexible casing coupling presented in Thorbjornsson et al. (2017), may avoid this dominating temperature effect and keep the design within yield. However, as discussed in Lohne et al. (2019), such designs are more appropriate to assess using RBD than WSD.

There is a big difference in the consequences of casing failure between offshore oil & gas activities and onshore geothermal activities. For offshore oil & gas where the casing is part of the barrier system, the regulations are stricter due to consequences related to explosions and environmental damages. In geothermal wells where the production casing is not necessarily considered part of a barrier system, the consequences are smaller. If regulations and environmental and safety consequences can be neglected in the analysis, then casing design can be reduced to mostly an economic evaluation. Such aspects work better within an RBD framework, where either target reliability levels, which is used as 0.5% in the examples in ISO/TR 10400 (2018) and dependent on consequences in Maes et al. (1995), or the full distribution can be used to evaluate the acceptability of designs.

6. CONCLUDING REMARKS

The analysis performed has been based on a triaxial model provided in API 5C3 TR (2018). Three-dimensional well tubular design is used both for working stress design calculations and following a reliability-based design approach to provide available pressure difference between the inside and outside of the casing. The model gives an accurate description of collapse below yield for the combination of inside pressure, outside pressure and axial stress, and should see increased use now that it has been included in API 5C3 TR (2018). The authors find it strange it was not included in the otherwise similar ISO/TR 10400 (2018) and was only referenced therein.

Through an example case the working stress design approach has been compared to a simplified reliability-based design approach. It illustrates that the design factors used for triaxial stress conditions are reasonable, but also that they do not fully reflect the risk associated with the design. In particular as activities progress to more difficult conditions (e.g. higher temperature and more corrosive downhole environment) a reliability-based approach can offer more information on what risk is taken and steps that can be taken to reduce it.

The approach has not been applied by the authors to any real cases, but it is an approach that allow for principles such as consistent treatment of risk, meaning that a risk level acceptable for a complex well should also be acceptable for another simpler well. Risk-based approaches, which reliability-based design is an example of, has seen increased use over many years in the oil and gas industry. Many regulators will in principle accept the use of such approaches (although what is required for it to be accepted is not always known). Regardless if risk-based design is acceptable by the regulators or not, the approach can create value within the confines of WSD acceptable designs through reduction in failures. In addition, reliability-based design can be used to generate different design factors that are relevant for specific well categories, which is important for geothermal wells due to the wide range of geological settings from which geothermal energy can be exploited.

REFERENCES

API TR 5C3 (2018): Calculating Performance Properties of Pipe Used as Casing or Tubing. *American Petroleum Institute Technical Report 5C3*, Washington, DC, Seventh Edition (June 2018)

Aasen, J.A., Ostvold, T.D. and Aadnoy, B.S.: Revitalized Three-Dimensional Design Method Improves Tubular Design., *Society of Petroleum Engineers*, Richardson, Texas (November 2017) SPE paper 188605

Das, B. and Samuel, R.: A Model for Well Reliability Analysis throughout the Life of a Well Using Barrier Engineering and Performance. *SPE/IADC Drilling Conference and Exhibition*, London, (2015) SPE/IADC-173055-MS

Davies, R. J., Almond, S., Ward, R. S., Jackson, R. B., Adams, C., Worrall, F., Herringshaw, L. G., Gluyas, J. G. and Whitehead, M. A.: Oil and gas wells and their integrity: Implications for shale and unconventional resource exploitation. *Marine and Petroleum Geology*, (2014), 239-254

Droessler, M., Curkan, B. and Hamilton, K.: Technical Considerations of Well Design and Equipment Selection for High Temperature Applications – A Canadian Perspective. *GRC Transactions*, 41, (2017)

Goodman, M. A., Kalil, I.A., McSpadden, A.R. and Coker III, O.D.: New Tubular-Design Ellipse With Backup Pressure. *SPE Drilling & Completion*, (2018), 149-164 (June)

ISO 14224: Petroleum, petrochemical and natural gas industries – Collection and exchange of reliability and maintenance data for equipment, *International Standard Organization*, Geneva, (2016)

ISO/TR 10400: Petroleum and natural gas industries - Formulae and calculations for the properties of casing, tubing, drill pipe and line pipe used as casing or tubing, *International Standard Organization*, Geneva, (2018)

Thorbjornsson, I., Kaldal, G. S., Gunnarsson, B. S. and Ragnarsson, Á.: A New Approach to Mitigate Casing failures in High-Temperature Geothermal Wells, *GRC Transactions*, 41, (2017)

Klinkenberg, A.: The Neutral Zones in Drill Pipe and Casing and Their Significance in Relation to Buckling and Collapse. *American Petroleum Institute Drilling Production Practice*, Dallas, Texas, (1951) 64-67

Kruszewski, M. and Wittig V.: Review of failure modes in supercritical geothermal drilling projects. *Geothermal Energy,* (2018), 6

Lewis, D. and Miller, R. A.: Casing design, in: Advanced Drilling and Well Technology, Aadnøy, B. S., Cooper, I. Miska, S. Z., Mitchell, R. F. and Payne, M. L. (Eds.), 153-166, *Society of Petroleum Engineers*, Richardson, TX, (2009)

Lohne, H. P., Randeberg, E., Ford, E. P. and Wildenborg, T.: Reliability analysis of new developed materials and technology, *GeoWell*, Stavanger, (2019)

Lubinski, A., Althouse, W.S. and Logan, J.L.: Helical Buckling of Tubing Sealed in Packers. *Journal of Petroleum Technology*, (1962), 655-670 (June)

Lubinski, A.: Influence of Neutral Axial Stress on Yield and Collapse of Pipe. *Journal of Engineering for Industry, Transactions of the ASME*, (1975), 400-407 (May)

Maes, M. A., Gulati, K. C., McKenna, D. L., Brand, P. R., Lewis, D. B. and Johnson, R. C.: Reliability-Based Casing Design. *Journal of Energy Resources Technology, Transactions of the ASME*, (1995), 93-100 (June)

NORSOK D-010: Well integrity in drilling and well operations. *Standards Norway*, Lysaker (2013)

NZS 2403: Code of Practice for Deep Geothermal Wells. *Standards New Zealand*, Wellington, NZ, (2015)

Sparks, C.P.: The Influence of Tension, Pressure and Weight on Pipe and Riser Deformations and Stresses. *Journal of Energy Resources Technology, Transactions of the ASME*, (1984), 46-54 (March)

Teodoriu, C.: Why and When Does Casing Fail in Geothermal Wells: a Surprising Question? *Proceedings World Geothermal Congress*, Melbourne, Australia, (April 2015)

Acknowledgements

Part of this work has been performed through the GeoWell project which has received funding from the European Union’s Horizon 2020 research and innovation programme under grant agreement No 654497